EUROPEAN JOURNAL OF PURE AND APPLIED MATHEMATICS
2025, Vol. 18, Issue 3, Article Number 6685
ISSN 1307-5543 – ejpam.com
Published by New York Business Global

Nonlinear Dynamics of Dengue Fever with Vaccination and Saturated Incidence

Mansoor Alsulami[1], Rashid Jan[2,3,4,*], Elisabeta Antonescu[5]

[1] *Department of Mathematics, Faculty of Science, King Abdulaziz University, P. O. Box 80203, Jeddah 21589, Saudi Arabia*
[2] *Department of Mathematics, Saveetha School of Engineering, SIMATS, Saveetha University, Chennai 602105, Tamil Nadu, India*
[3] *Department of Mathematics, Khazar University, AZ1096, Baku, Azerbaijan*
[4] *Institute of Energy Infrastructure (IEI), Department of Civil Engineering, College of Engineering, Universiti Tenaga Nasional (UNITEN), Putrajaya Campus, Jalan IKRAM-UNITEN, 43000 Kajang, Selangor, Malaysia*
[5] *Preclinical Department Faculty of Medicine, Lucian Blaga University of Sibiu, Sibiu, Romania*

Abstract. Dengue fever is a viral disease that presents serious public health challenges worldwide. Its burden is especially pronounced in resource-limited or underserved regions, where it leads to considerable social and economic consequences. In this study, we model the dynamics of dengue by incorporating the effects of vaccination and treatment using the fractal-fractional Caputo derivative. Additionally, a saturated incidence rate is assumed to more accurately represent the dynamics of the infection. The basic reproduction number, $\mathcal{R}_0$, is derived using the next-generation matrix method to assess the potential for disease persistence or eradication. Numerical simulations, conducted using a reliable computational scheme, evaluate the influence of various biological and intervention-related parameters on the outbreak's progression. The results highlight the critical roles of vaccination, transmission rate, and treatment in shaping the epidemic curve. This analysis identifies key parameters that most significantly impact disease dynamics, providing valuable insights for public health authorities to optimize intervention strategies aimed at reducing dengue transmission and mitigating outbreak severity.

2020 Mathematics Subject Classifications: 92D25, 92D30

Key Words and Phrases: Dengue infection, fractal-fractional dynamics, Saturated incidence, Numerical analysis, Dynamical behaviour

*Corresponding author.
DOI: https://doi.org/10.29020/nybg.ejpam.v18i3.6685

Email addresses: maalsulami2@kau.edu.sa (M. Alsulami), rashid_ash2000@yahoo.com (R. Jan), elisabeta.antonescu@ulbsibiu.ro (E. Antonescu)

1. Introduction

Dengue fever is a mosquito-borne infection predominantly found in tropical areas. An infected female *Aedes* mosquito transmits the virus to the blood of a human host during feeding [1]. Typical symptoms of dengue include high-grade fever, severe headaches, joint and muscle pain, skin rashes, and, in severe cases, bleeding complications. It is worth noting that rare cases of vertical transmission have been reported in both species. Preventative measures for dengue infection include mosquito control, such as the elimination of breeding sites and the use of insect repellents and bed nets [2, 3]. There is ongoing research into the development of vaccines and antiviral treatments to combat dengue infection. Dengue prevention strategies primarily focus on vector control, public education, and disease surveillance to reduce viral transmission. It is widely recognized that no fully effective vaccine for dengue fever currently exists, although a partially effective vaccine is available in some regions [4, 5]. Additionally, various vaccines for dengue infection have been developed and are undergoing clinical testing, as reported in references [6, 7]. Consequently, alternative preventive measures are essential to manage and mitigate the prevalence of dengue infection.

Mathematical innovations continue to facilitate the formulation, analysis, and optimization of complex systems in interdisciplinary scientific research [8–10]. Mathematical models serve as valuable tools for the exploration diseases and the introduction of effective strategies for infection control [11, 12]. These models identify and emphasize the most critical and influential factors for the spread and management [13]. Over the past decades, numerous models have been developed to investigate the transmission dynamics and epidemiological characteristics of dengue [14–20]. Lourdes Esteva, for instance, developed the foundational model for dengue fever, exploring its behavior within a variable human population [14, 15]. In 1997, researchers formulated and analyzed a two-strain model to better understand the disease dynamics [18]. Additionally, other researchers have introduced models for dengue fever and investigated the stability of their systems, as documented in their work [16, 20]. Furthermore, researchers have delved into the dynamics of dengue, considering the impact of vaccination and antibody-dependent enhancement (ADE) phenomena to gain insights into disease transmission [21–23]. In the existing literature, a common approach to control vector-borne diseases involves two primary interventions: one targeting human immunization and the other focused on mosquito population reduction [24–28]. These models primarily concentrate on vaccination, larvicidal, and adulticidal measures as key strategies in combating the disease. Further advancements and continued research are essential to effectively capture and manage the complex dynamics of dengue fever.

Fractal dynamics significantly contribute to improving the realism and predictive capability of epidemic models, particularly for complex infectious diseases [29–31]. However, the fractal-fractional framework is more comprehensive, as it incorporates both memory effects and spatial heterogeneity. The memory effect, embedded in fractional calculus, allows the model to account for past states of the system, capturing long-term biological and environmental influences [32–34]. Simultaneously, the fractal component reflects the

irregular, self-similar structures often observed in the spatial spread of infections due to varying human mobility patterns, environmental factors, and heterogeneous population densities. This dual capability makes fractal-fractional models highly adaptable to real-world data, enabling them to replicate epidemic curves with features like sub-exponential growth, multiple waves, and long tails. Moreover, these models provide a generalized framework that encompasses classical models as special cases, offering greater flexibility in parameter tuning and scenario analysis. Their ability to simulate the impact of vaccination and other control strategies over time, while considering the cumulative effect of past interventions, makes them an invaluable tool for public health planning and epidemic management.

The structure of this research is as: A mathematical model describing the dynamics of dengue, incorporating treatment and vaccination, has been developed in Section 2. In Section 3, the foundational concepts and key properties of the fractal-fractional derivative are introduced. In Section 4, the threshold parameter of the system is determined. A suitable numerical scheme for solving the proposed fractal-fractional model is detailed in Section 5, along with a comprehensive investigation of the system's dynamical behavior through simulations. Finally, the main findings and conclusions are summarized in the concluding section.

2. Evaluation of the model

Let the total populations of vectors and hosts be denoted by $\mathscr{N}_v$ and $\mathscr{N}_h$, respectively. The total female mosquito population $\mathscr{N}_v$ is classified into susceptible $\mathscr{S}_v$ and infected $\mathscr{I}_v$ vectors. Similarly, the total host population $\mathscr{N}_h$ is classified into susceptible $\mathscr{S}_h$, vaccinated $\mathscr{V}_h$, infected $\mathscr{I}_h$, and recovered $\mathscr{R}_h$ individuals. We also supposed that both the hosts and vectors experience natural birth and death at constant rates denoted by μ_h and μ_v, respectively. The disease-induced mortality is negligible and thus excluded from the model.

To capture transmission dynamics more realistically, we incorporate *nonlinear forces of infection* governed by saturated incidence rates. Specifically, the transmission of dengue from I_v to susceptible and $\mathscr{V}_h$ is represented by the terms

$$\frac{b\beta_1}{1+\alpha_h\mathscr{I}_v}\mathscr{S}_h\mathscr{I}_v \quad \text{and} \quad \frac{b\beta_2}{1+\alpha_h\mathscr{I}_v}\mathscr{V}_h\mathscr{I}_v,$$

respectively. Transmission from infected hosts to S_v is modeled by

$$\frac{b\beta_3}{1+\alpha_v\mathscr{I}_h}\mathscr{S}_v\mathscr{I}_h,$$

in which b is the average biting rate, β_i (for $i=1,2,3$) are the transmission probabilities per bite, and α_h, α_v are the saturation parameters reflecting behavioral or physiological limitations in contact rates. Vaccination is assumed to confer immediate protection to a fraction p of the susceptible $\mathscr{S}_h$, who transition to the vaccinated class $\mathscr{V}_h$. Additionally,

it is assumed that a fraction ν returns to $\mathscr{S}_h$ after losing immunity. Based on these assumptions, the dynamics of dengue are represented by:

$$\begin{cases} \frac{d\mathscr{S}_h}{dt} &= \Lambda_h - \frac{b\beta_1}{1+\alpha_h\mathscr{I}_v}\mathscr{S}_h\mathscr{I}_v - \mu_h\mathscr{S}_h - p\mathscr{S}_h + \upsilon\mathscr{R}_h, \\ \frac{d\mathscr{V}_h}{dt} &= p\mathscr{S}_h - \frac{b\beta_2}{1+\alpha_h\mathscr{I}_v}\mathscr{V}_h\mathscr{I}_v - \mu_h\mathscr{V}_h, \\ \frac{d\mathscr{I}_h}{dt} &= \frac{b\beta_1}{1+\alpha_h\mathscr{I}_v}\mathscr{S}_h\mathscr{I}_v + \frac{b\beta_2}{1+\alpha_h\mathscr{I}_v}\mathscr{V}_h\mathscr{I}_v - (\mu_h+\gamma_h+\tau)\mathscr{I}_h, \\ \frac{d\mathscr{R}_h}{dt} &= \gamma_h\mathscr{I}_h + \tau\mathscr{I}_h - \upsilon\mathscr{R}_h - \mu_h\mathscr{R}_h, \\ \frac{d\mathscr{S}_v}{dt} &= \Lambda_v - \frac{\beta_3 b}{1+\alpha_v\mathscr{I}_h}\mathscr{S}_v\mathscr{I}_h - \mu_v\mathscr{S}_v, \\ \frac{d\mathscr{I}_v}{dt} &= \frac{b\beta_3}{1+\alpha_v\mathscr{I}_h}\mathscr{S}_v\mathscr{I}_h - \mu_v\mathscr{I}_v, \end{cases} \tag{1}$$

with the following

$$0 \le \mathscr{S}_v(0), 0 \le \mathscr{I}_v(0), 0 \le \mathscr{S}_h(0), 0 \le \mathscr{V}_h(0), 0 \le \mathscr{I}_h(0), 0 \le \mathscr{R}_h(0),$$

where the parameter $\alpha_h \in [0,1]$ symbolize the responsiveness rate of antibodies produced in humans in reaction to antigens introduced by infectious vectors, while $\alpha_v \in [0,1]$ denotes the rate at which antibodies are generated in vectors upon contact with antigens from infectious human hosts. In the subsequent analysis, we investigate the recommended model (1) of dengue for biologically feasible region.

Theorem 1. *The closed set defined by* $\Omega = \{(\mathscr{S}_h, \mathscr{V}_h, \mathscr{I}_h, \mathscr{R}_h, \mathscr{S}_v, \mathscr{I}_v) \in R_+^6 : 0 \le \mathscr{S}_h + \mathscr{V}_h + \mathscr{I}_h + \mathscr{R}_h \le \frac{\Lambda_h}{\mu_h}, 0 \le \mathscr{S}_v + \mathscr{I}_v \le \frac{\Lambda_v}{\mu_v}\}$ *is a positive invariant set for the recommended dengue system (2).*

The incorporation of fractal-fractional dynamics into the modeling of dengue fever offers a powerful and comprehensive framework for capturing the complex, memory-dependent processes inherent in disease transmission. Fractal-fractional models account for the non-local behavior and long-term memory effects present in both host and vector populations. Thus, we represent the proposed dynamics through fractal-fractional derivative as

$$\begin{cases} {}_0^{FF}D_t^{\rho,\kappa}\mathscr{S}_h &= \Lambda_h - \frac{b\beta_1}{1+\alpha_h\mathscr{I}_v}\mathscr{S}_h\mathscr{I}_v - \mu_h\mathscr{S}_h - p\mathscr{S}_h + \upsilon\mathscr{R}_h, \\ {}_0^{FF}D_t^{\rho,\kappa}\mathscr{V}_h &= p\mathscr{S}_h - \frac{b\beta_2}{1+\alpha_h\mathscr{I}_v}\mathscr{V}_h\mathscr{I}_v - \mu_h\mathscr{V}_h, \\ {}_0^{FF}D_t^{\rho,\kappa}\mathscr{I}_h &= \frac{b\beta_1}{1+\alpha_h\mathscr{I}_v}\mathscr{S}_h\mathscr{I}_v + \frac{b\beta_2}{1+\alpha_h\mathscr{I}_v}\mathscr{V}_h\mathscr{I}_v - (\mu_h+\gamma_h+\tau)\mathscr{I}_h, \\ {}_0^{FF}D_t^{\rho,\kappa}\mathscr{R}_h &= \gamma_h\mathscr{I}_h + \tau\mathscr{I}_h - \upsilon\mathscr{R}_h - \mu_h\mathscr{R}_h, \\ {}_0^{FF}D_t^{\rho,\kappa}\mathscr{S}_v &= \Lambda_v - \frac{\beta_3 b}{1+\alpha_v\mathscr{I}_h}\mathscr{S}_v\mathscr{I}_h - \mu_v\mathscr{S}_v, \\ {}_0^{FF}D_t^{\rho,\kappa}\mathscr{I}_v &= \frac{b\beta_3}{1+\alpha_v\mathscr{I}_h}\mathscr{S}_v\mathscr{I}_h - \mu_v\mathscr{I}_v, \end{cases} \tag{2}$$

where ${}_0^{FF}D_t^{\rho,\kappa}$ denotes the Caputo fractal-fractional derivative with fractal and fractional orders κ and ρ, respectively. By providing a more realistic and flexible mathematical representation of dengue dynamics, fractal-fractional models contribute significantly to the development of effective public health policies and improve the alignment between theoretical predictions and empirical data.

3. Theory and results

Here, we will present some basic theory and results of fractal-fractional derivative for the analysis of subsequent work [35, 36].

Definition 1. *Assume a function $x(t)$ such that $x(t)$ be continuous and differentiable on (a,b), and let κ denote its fractal order. The* fractal-fractional derivative *of $x(t)$ of order ρ in the Riemann–Liouville sense with a power-law kernel is defined as*

$$^{FFP}D_{0,t}^{\rho,\kappa}\big(x(t)\big) = \frac{1}{\Gamma(m-\rho)}\frac{d}{dt^{\kappa}}\int_0^t (t-s)^{m-\rho-1}x(s)\,ds, \tag{3}$$

where $m \in \mathbb{N}$ such that $m-1 < \rho, \kappa \leq m$. Here, the fractal derivative is denoted by $\frac{d}{dt^{\kappa}}$ of order κ and is

$$\frac{dx(s)}{ds^{\kappa}} = \lim_{t\to s}\frac{x(t)-x(s)}{t^{\kappa}-s^{\kappa}}. \tag{4}$$

Definition 2. *Let $x(t)$ be a function that is both continuous and admits a fractal derivative of order κ on the interval (a,b). The Riemann–Liouville fractal-fractional derivative of $x(t)$ with an exponential kernel of order ρ is given by*

$$^{\text{FFE}}D_{0,t}^{\rho,\kappa}\left(x(t)\right) = \frac{M(\rho)}{1-\rho}\frac{d}{dt^{\kappa}}\int_0^t \exp\left(-\frac{\rho}{1-\rho}(t-s)\right)x(s)\,ds, \tag{5}$$

where $\rho \in (0,1)$, $\kappa \leq m$, with $m \in \mathbb{N}$, and $M(\rho)$ is a normalization factor satisfying

$$M(0) = M(1) = 1.$$

Definition 3. *Let $x(t)$ be continuous and fractal-differentiable on the interval (a,b), where κ denotes the order of fractal differentiation. The fractal-fractional derivative of $x(t)$ of order ρ in the Riemann-Liouville sense with a generalized Mittag-Leffler kernel is*

$$^{FFM}D_{0,t}^{\rho,\kappa}\big(x(t)\big) = \frac{AB(\rho)}{1-\rho}\frac{d}{dt^{\kappa}}\int_0^t E_{\rho}\left(-(t-s)^{\rho}\frac{\rho}{1-\rho}\right)x(s)\,ds, \tag{6}$$

where $0 < \rho$, $\kappa \leq 1$, $\kappa \in \mathbb{N}$, and

$$AB(\rho) = \frac{\rho}{\Gamma(\rho)} + 1 - \rho.$$

Here, $E_{\rho}(\cdot)$ denotes the Mittag-Leffler function.

Definition 4. *Let $x(t)$ be a continuous function defined on (a,b). The fractal-fractional integral of order ρ of the function $x(t)$, characterized by a power-law kernel is given by*

$$^{FFP}J_{0,t}^{\rho}\big(x(t)\big) = \frac{\kappa}{\Gamma(\rho)}\int_0^t (t-s)^{\rho-1}s^{\kappa-1}x(s)\,ds, \tag{7}$$

where $\rho > 0$ and $\kappa > 0$.

Definition 5. *Suppose a continuous function $x(t)$ on (a,b). Then, the integral with exponentially decay kernel is*

$$ {}^{FFE}J^{\rho}_{0,t}\big(x(t)\big) = \frac{\rho\kappa}{M(\rho)}\int_0^t s^{\rho-1}x(s)\,ds + \frac{\kappa(1-\rho)t^{\kappa-1}x(t)}{M(\rho)}. \tag{8}$$

Definition 6. *The generalized Mittag-Leffler kernel for a continuous function $x(t)$ for the above operator with order κ and ρ is given by*

$$ {}^{FFM}J^{\rho,\kappa}_{0,t}\big(x(t)\big) = \frac{\rho\kappa}{AB(\rho)}\int_0^t s^{\kappa-1}(t-s)^{\rho-1}x(s)\,ds + \frac{\kappa(1-\rho)t^{\kappa-1}x(t)}{AB(\rho)}, \tag{9}$$

where $AB(\rho)$ denotes a normalization function associated with the kernel.

3.1. Threshold parameter

In this subsection, we derive the disease-free equilibrium (DFE) of the proposed dengue transmission model, followed by the computation of the associated threshold parameter, commonly referred to as the basic reproduction number. To determine the equilibria of the system, we begin by considering the model equations in the following form:

$$\begin{cases} 0 &= \Lambda_h - \frac{b\beta_1}{1+\alpha_h\mathscr{I}_v}\mathscr{S}_h\mathscr{I}_v - \mu_h\mathscr{S}_h - p\mathscr{S}_h + \upsilon\mathscr{R}_h,\\ 0 &= p\mathscr{S}_h - \frac{b\beta_2}{1+\alpha_h\mathscr{I}_v}\mathscr{V}_h\mathscr{I}_v - \mu_h\mathscr{V}_h,\\ 0 &= \frac{b\beta_1}{1+\alpha_h\mathscr{I}_v}\mathscr{S}_h\mathscr{I}_v + \frac{b\beta_2}{1+\alpha_h\mathscr{I}_v}\mathscr{V}_h\mathscr{I}_v - (\mu_h+\gamma_h+\tau)\mathscr{I}_h,\\ 0 &= \gamma_h\mathscr{I}_h + \tau\mathscr{I}_h - \upsilon\mathscr{R}_h - \mu_h\mathscr{R}_h,\\ 0 &= \Lambda_v - \frac{\beta_3 b}{1+\alpha_v\mathscr{I}_h}\mathscr{S}_v\mathscr{I}_h - \mu_v\mathscr{S}_v,\\ 0 &= \frac{b\beta_3}{1+\alpha_v\mathscr{I}_h}\mathscr{S}_v\mathscr{I}_h - \mu_v\mathscr{I}_v. \end{cases} \tag{10}$$

For disease-free equilibrium, we take $\mathscr{I}_h = 0$ and $\mathscr{I}_v = 0$ in the above and get

$$\mathcal{E}_0(\mathscr{S}_h^0, \mathscr{V}_h^0, \mathscr{I}_h^0, \mathscr{R}_h^0, \mathscr{S}_v^0, \mathscr{I}_v^0) = \left(\frac{\Lambda_h}{p+\mu_h}, \frac{\Lambda_h p}{(p+\mu_h)\mu_h}, 0, 0, \frac{\Lambda_v}{\mu_v}, 0\right).$$

To determine the threshold parameter, we will use the concept outlined in the research work [37, 38] which is symbolized by $\mathcal{R}_0$ and is find out as

$$\mathcal{F} = \begin{bmatrix} \frac{b\beta_1}{1+\alpha_h\mathscr{I}_v}\mathscr{S}_h\mathscr{I}_v + \frac{b\beta_2}{1+\alpha_h\mathscr{I}_v}\mathscr{V}_h\mathscr{I}_v \\ \frac{b\beta_3}{1+\alpha_v\mathscr{I}_h}\mathscr{S}_v\mathscr{I}_h \end{bmatrix} \text{ and } \mathcal{V} = \begin{bmatrix} (\mu_h+\gamma_h+\tau)\mathscr{I}_h \\ \mu_v\mathscr{I}_v \end{bmatrix},$$

which further implies the following

$$\mathrm{F} = \begin{bmatrix} 0 & b\beta_1\mathscr{S}_h^0 + b\beta_2\mathscr{V}_h^0 \\ b\beta_3\mathscr{S}_v^0 & 0 \end{bmatrix} \text{ and } \mathrm{V} = \begin{bmatrix} \mu_h+\gamma_h+\tau & 0 \\ 0 & \mu_v \end{bmatrix},$$

next, we have

$$\mathrm{FV}^{-1} = \begin{bmatrix} 0 & \frac{b\beta_1\mathscr{S}_h^0 + b\beta_2\mathscr{V}_h^0}{\mu_v} \\ \frac{b\beta_3\mathscr{S}_v^0}{\mu_h+\gamma_h+\tau} & 0 \end{bmatrix}.$$

The spectral radius of the above FV^{-1} is denoted by $\rho(FV^{-1})$ and is given by

$$\rho(FV^{-1}) = \sqrt{\frac{b\beta_3\mathscr{S}_v^0}{(\mu_h+\gamma_h+\tau)\mu_v}\left(b\beta_1\mathscr{S}_h^0 + b\beta_2\mathscr{V}_h^0\right)},$$

this implies the following

$$\mathcal{R}_0 = \sqrt{\frac{b\beta_3\Lambda_v\Lambda_h}{(\mu_h+\gamma_h)\mu_v\mu_v}\left(\frac{b\beta_1}{(p+\mu_h)} + \frac{b\beta_2 p}{(p+\mu_h)\mu_h}\right)}.$$

4. Numerical scheme and analysis

In this section, we present a novel numerical method for the fractal-fractional Caputo (FFC) system (2) describing dengue infection dynamics. To facilitate the numerical procedure, the FFC system is first reformulated as an equivalent Volterra-type integral equation. Consequently, the system involving the FFC derivative can be represented as follows:

$$\frac{1}{\Gamma(1-\rho)}\frac{d}{dt}\int_0^t (t-\kappa)^\rho f(\kappa)d\kappa\frac{1}{\kappa t^{\kappa-1}}, \tag{11}$$

thus, the below is obtained

$$\begin{aligned}
{}^{RL}D^\rho_{0,t}\mathscr{S}_h &= \kappa t^{\kappa-1}\big(\Lambda_h - \frac{b\beta_1}{1+\alpha_h\mathscr{I}_v}\mathscr{S}_h\mathscr{I}_v - \mu_h\mathscr{S}_h - p\mathscr{S}_h + \upsilon\mathscr{R}_h\big),\\
{}^{RL}D^\rho_{0,t}\mathscr{V}_h &= \kappa t^{\kappa-1}\big(p\mathscr{S}_h - \frac{b\beta_2}{1+\alpha_h\mathscr{I}_v}\mathscr{V}_h\mathscr{I}_v - \mu_h\mathscr{V}_h\big),\\
{}^{RL}D^\rho_{0,t}\mathscr{I}_h &= \kappa t^{\kappa-1}\big(\frac{b\beta_1}{1+\alpha_h\mathscr{I}_v}\mathscr{S}_h\mathscr{I}_v + \frac{b\beta_2}{1+\alpha_h\mathscr{I}_v}\mathscr{V}_h\mathscr{I}_v - (\mu_h+\gamma_h+\tau)\mathscr{I}_h\big),\\
{}^{RL}D^\rho_{0,t}\mathscr{R}_h &= \kappa t^{\kappa-1}\big(\gamma_h\mathscr{I}_h + \tau\mathscr{I}_h - \upsilon\mathscr{R}_h - \mu_h\mathscr{R}_h\big),\\
{}^{RL}D^\rho_{0,t}\mathscr{S}_v &= \kappa t^{\kappa-1}\big(\Lambda_v - \frac{\beta_3 b}{1+\alpha_v\mathscr{I}_h}\mathscr{S}_v\mathscr{I}_h - \mu_v\mathscr{S}_v\big),\\
{}^{RL}D^\rho_{0,t}\mathscr{I}_v &= \kappa t^{\kappa-1}\big(\frac{b\beta_3}{1+\alpha_v\mathscr{I}_h}\mathscr{S}_v\mathscr{I}_h - \mu_v\mathscr{I}_v\big).
\end{aligned} \tag{12}$$

To make the Riemann-Liouville derivative flexible for the beginning circumstances, we convert it to the Caputo derivative. Applying the fractional integral in the following step yields the following

$$\mathscr{S}_h(t) = \mathscr{S}_h(0) + \frac{\kappa}{\Gamma(\rho)}\int_0^t \xi^{\kappa-1}(t-\xi)^{\rho-1}g_1(\mathscr{S}_h,\mathscr{V}_h,\mathscr{I}_h,\mathscr{R}_h,\mathscr{S}_v,\mathscr{I}_v,\xi)d\xi,$$

$$
\begin{aligned}
\mathscr{V}_h(t) &= \mathscr{V}_h(0) + \frac{\kappa}{\Gamma(\rho)} \int_0^t \xi^{\kappa-1}(t-\xi)^{\rho-1} g_2(\mathscr{S}_h, \mathscr{V}_h, \mathscr{I}_h, \mathscr{R}_h, \mathscr{S}_v, \mathscr{I}_v, \xi) d\xi, \\
\mathscr{I}_h(t) &= \mathscr{I}_h(0) + \frac{\kappa}{\Gamma(\rho)} \int_0^t \xi^{\kappa-1}(t-\xi)^{\rho-1} g_3(\mathscr{S}_h, \mathscr{V}_h, \mathscr{I}_h, \mathscr{R}_h, \mathscr{S}_v, \mathscr{I}_v, \xi) d\xi, \\
\mathscr{R}_h(t) &= \mathscr{R}_h(0) + \frac{\kappa}{\Gamma(\rho)} \int_0^t \xi^{\kappa-1}(t-\xi)^{\rho-1} g_4(\mathscr{S}_h, \mathscr{V}_h, \mathscr{I}_h, \mathscr{R}_h, \mathscr{S}_v, \mathscr{I}_v, \xi) d\xi, \\
\mathscr{S}_v(t) &= \mathscr{S}_v(0) + \frac{\kappa}{\Gamma(\rho)} \int_0^t \xi^{\kappa-1}(t-\xi)^{\rho-1} g_5(\mathscr{S}_h, \mathscr{V}_h, \mathscr{I}_h, \mathscr{R}_h, \mathscr{S}_v, \mathscr{I}_v, \xi) d\xi, \\
\mathscr{I}_v(t) &= \mathscr{I}_v(0) + \frac{\kappa}{\Gamma(\rho)} \int_0^t \xi^{\kappa-1}(t-\xi)^{\rho-1} g_6(\mathscr{S}_h, \mathscr{V}_h, \mathscr{I}_h, \mathscr{R}_h, \mathscr{S}_v, \mathscr{I}_v, \xi) d\xi, \qquad (13)
\end{aligned}
$$

where

$$
\begin{aligned}
g_1(\mathscr{S}_h, \mathscr{V}_h, \mathscr{I}_h, \mathscr{R}_h, \mathscr{S}_v, \mathscr{I}_v, \xi) &= \Lambda_h - \frac{b\beta_1}{1+\alpha_h \mathscr{I}_v} \mathscr{S}_h \mathscr{I}_v - \mu_h \mathscr{S}_h - p\mathscr{S}_h + \upsilon \mathscr{R}_h, \\
g_2(\mathscr{S}_h, \mathscr{V}_h, \mathscr{I}_h, \mathscr{R}_h, \mathscr{S}_v, \mathscr{I}_v, \xi) &= p\mathscr{S}_h - \frac{b\beta_2}{1+\alpha_h \mathscr{I}_v} \mathscr{V}_h \mathscr{I}_v - \mu_h \mathscr{V}_h, \\
g_3(\mathscr{S}_h, \mathscr{V}_h, \mathscr{I}_h, \mathscr{R}_h, \mathscr{S}_v, \mathscr{I}_v, \xi) &= \frac{b\beta_1}{1+\alpha_h \mathscr{I}_v} \mathscr{S}_h \mathscr{I}_v + \frac{b\beta_2}{1+\alpha_h \mathscr{I}_v} \mathscr{V}_h \mathscr{I}_v - (\mu_h + \gamma_h + \tau) \mathscr{I}_h, \\
g_4(\mathscr{S}_h, \mathscr{V}_h, \mathscr{I}_h, \mathscr{R}_h, \mathscr{S}_v, \mathscr{I}_v, \xi) &= \gamma_h \mathscr{I}_h + \tau \mathscr{I}_h - \upsilon \mathscr{R}_h - \mu_h \mathscr{R}_h, \\
g_5(\mathscr{S}_h, \mathscr{V}_h, \mathscr{I}_h, \mathscr{R}_h, \mathscr{S}_v, \mathscr{I}_v, \xi) &= \Lambda_v - \frac{\beta_3 b}{1+\alpha_v \mathscr{I}_h} \mathscr{S}_v \mathscr{I}_h - \mu_v \mathscr{S}_v, \\
g_6(\mathscr{S}_h, \mathscr{V}_h, \mathscr{I}_h, \mathscr{R}_h, \mathscr{S}_v, \mathscr{I}_v, \xi) &= \frac{b\beta_3}{1+\alpha_v \mathscr{I}_h} \mathscr{S}_v \mathscr{I}_h - \mu_v \mathscr{I}_v.
\end{aligned}
$$

Here, at time t_{m+1}, we obtain

$$
\begin{aligned}
\mathscr{S}_h(t) &= \mathscr{S}_h(0) + \frac{\kappa}{\Gamma(\rho)} \int_0^t \xi^{\kappa-1}(t_{n+1}-\xi)^{\rho-1} g_1(\mathscr{S}_h, \mathscr{V}_h, \mathscr{I}_h, \mathscr{R}_h, \mathscr{S}_v, \mathscr{I}_v, \xi) d\xi, \\
\mathscr{V}_h(t) &= \mathscr{V}_h(0) + \frac{\kappa}{\Gamma(\rho)} \int_0^t \xi^{\kappa-1}(t_{n+1}-\xi)^{\rho-1} g_2(\mathscr{S}_h, \mathscr{V}_h, \mathscr{I}_h, \mathscr{R}_h, \mathscr{S}_v, \mathscr{I}_v, \xi) d\xi, \\
\mathscr{I}_h(t) &= \mathscr{I}_h(0) + \frac{\kappa}{\Gamma(\rho)} \int_0^t \xi^{\kappa-1}(t_{n+1}-\xi)^{\rho-1} g_3(\mathscr{S}_h, \mathscr{V}_h, \mathscr{I}_h, \mathscr{R}_h, \mathscr{S}_v, \mathscr{I}_v, \xi) d\xi, \\
\mathscr{R}_h(t) &= \mathscr{R}_h(0) + \frac{\kappa}{\Gamma(\rho)} \int_0^t \xi^{\kappa-1}(t_{n+1}-\xi)^{\rho-1} g_4(\mathscr{S}_h, \mathscr{V}_h, \mathscr{I}_h, \mathscr{R}_h, \mathscr{S}_v, \mathscr{I}_v, \xi) d\xi, \\
\mathscr{S}_v(t) &= R_v(0) + \frac{\kappa}{\Gamma(\rho)} \int_0^t \xi^{\kappa-1}(t_{n+1}-\xi)^{\rho-1} g_5(\mathscr{S}_h, \mathscr{V}_h, \mathscr{I}_h, \mathscr{R}_h, \mathscr{S}_v, \mathscr{I}_v, \xi) d\xi, \\
\mathscr{I}_v(t) &= \mathscr{I}_v(0) + \frac{\kappa}{\Gamma(\rho)} \int_0^t \xi^{\kappa-1}(t_{n+1}-\xi)^{\rho-1} g_6(\mathscr{S}_h, \mathscr{V}_h, \mathscr{I}_h, \mathscr{R}_h, \mathscr{S}_v, \mathscr{I}_v, \xi) d\xi. \qquad (14)
\end{aligned}
$$

Approximation of (14) implies

$$\begin{aligned}
\mathscr{S}_h^{m+1} &= \mathscr{S}_h^0 + \frac{\kappa}{\Gamma(\rho)}\sum_{j=0}^{m}\int_{t_j}^{t_{j+1}} \xi^{\kappa-1}(t_{m+1}-\xi)^{\rho-1} g_1(\mathscr{S}_h, \mathscr{V}_h, \mathscr{I}_h, \mathscr{R}_h, \mathscr{S}_v, \mathscr{I}_v, \xi)d\xi,\\
\mathscr{V}_h^{m+1} &= \mathscr{V}_h^0 + \frac{\kappa}{\Gamma(\rho)}\sum_{j=0}^{m}\int_{t_j}^{t_{j+1}} \xi^{\kappa-1}(t_{m+1}-\xi)^{\rho-1} g_2(\mathscr{S}_h, \mathscr{V}_h, \mathscr{I}_h, \mathscr{R}_h, \mathscr{S}_v, \mathscr{I}_v, \xi)d\xi,\\
\mathscr{I}_h^{m+1} &= \mathscr{I}_h^0 + \frac{\kappa}{\Gamma(\rho)}\sum_{j=0}^{m}\int_{t_j}^{t_{j+1}} \xi^{\kappa-1}(t_{m+1}-\xi)^{\rho-1} g_3(\mathscr{S}_h, \mathscr{V}_h, \mathscr{I}_h, \mathscr{R}_h, \mathscr{S}_v, \mathscr{I}_v, \xi)d\xi,\\
\mathscr{R}_h^{m+1} &= \mathscr{R}_h^0 + \frac{\kappa}{\Gamma(\rho)}\sum_{j=0}^{m}\int_{t_j}^{t_{j+1}} \xi^{\kappa-1}(t_{m+1}-\xi)^{\rho-1} g_4(\mathscr{S}_h, \mathscr{V}_h, \mathscr{I}_h, \mathscr{R}_h, \mathscr{S}_v, \mathscr{I}_v, \xi)d\xi,\\
\mathscr{S}_v^{m+1} &= \mathscr{S}_v^0 + \frac{\kappa}{\Gamma(\rho)}\sum_{j=0}^{m}\int_{t_j}^{t_{j+1}} \xi^{\kappa-1}(t_{m+1}-\xi)^{\rho-1} g_5(\mathscr{S}_h, \mathscr{V}_h, \mathscr{I}_h, \mathscr{R}_h, \mathscr{S}_v, \mathscr{I}_v, \xi)d\xi,\\
\mathscr{I}_v^{m+1} &= \mathscr{I}_v^0 + \frac{\kappa}{\Gamma(\rho)}\sum_{j=0}^{m}\int_{t_j}^{t_{j+1}} \xi^{\kappa-1}(t_{m+1}-\xi)^{\rho-1} g_6(\mathscr{S}_h, \mathscr{V}_h, \mathscr{I}_h, \mathscr{R}_h, \mathscr{S}_v, \mathscr{I}_v, \xi)d\xi. \quad (15)
\end{aligned}$$

Additionally, the function $\xi^{\kappa-1}g_1(\mathscr{S}_h, \mathscr{V}_h, \mathscr{I}_h, \mathscr{R}_h, \mathscr{S}_v, \mathscr{I}_v, \xi)$ on the interval $[t_j, t_{j+1}]$ is approximated with the help of the Lagrangian piece-wise interpolation as:

$$\begin{aligned}
P_j(\xi) &= \frac{\xi - t_{j-1}}{t_j - t_{j-1}} t_j^{\kappa-1} g_1\big(\mathscr{S}_h^j, \mathscr{V}_h^j, \mathscr{I}_h^j, \mathscr{R}_h^j, \mathscr{S}_v^j, \mathscr{I}_v^j, t_j\big)\\
&- \frac{\xi - t_j}{t_j - t_{j-1}} t_{j-1}^{\kappa-1} g_1\big(\mathscr{S}_h^{j-1}, \mathscr{V}_h^{j-1}, \mathscr{I}_h^{j-1}, \mathscr{R}_h^{j-1}, \mathscr{S}_v^{j-1}, \mathscr{I}_v^{j-1}, t_{j-1}\big),\\
Q_j(\xi) &= \frac{\xi - t_{j-1}}{t_j - t_{j-1}} t_j^{\kappa-1} g_2\big(\mathscr{S}_h^j, \mathscr{V}_h^j, \mathscr{I}_h^j, \mathscr{R}_h^j, \mathscr{S}_v^j, \mathscr{I}_v^j, t_j\big)\\
&- \frac{\xi - t_j}{t_j - t_{j-1}} t_{j-1}^{\kappa-1} g_2\big(\mathscr{S}_h^{j-1}, \mathscr{V}_h^{j-1}, \mathscr{I}_h^{j-1}, \mathscr{R}_h^{j-1}, \mathscr{S}_v^{j-1}, \mathscr{I}_v^{j-1}, t_{j-1}\big),\\
R_j(\xi) &= \frac{\xi - t_{j-1}}{t_j - t_{j-1}} t_j^{\kappa-1} g_3\big(\mathscr{S}_h^j, \mathscr{V}_h^j, \mathscr{I}_h^j, \mathscr{R}_h^j, \mathscr{S}_v^j, \mathscr{I}_v^j, t_j\big)\\
&- \frac{\xi - t_j}{t_j - t_{j-1}} t_{j-1}^{\kappa-1} g_3\big(\mathscr{S}_h^{j-1}, \mathscr{V}_h^{j-1}, \mathscr{I}_h^{j-1}, \mathscr{R}_h^{j-1}, \mathscr{S}_v^{j-1}, \mathscr{I}_v^{j-1}, t_{j-1}\big),\\
S_j(\xi) &= \frac{\xi - t_{j-1}}{t_j - t_{j-1}} t_j^{\kappa-1} g_4\big(\mathscr{S}_h^j, \mathscr{V}_h^j, \mathscr{I}_h^j, \mathscr{R}_h^j, \mathscr{S}_v^j, \mathscr{I}_v^j, t_j\big)\\
&- \frac{\xi - t_j}{t_j - t_{j-1}} t_{j-1}^{\kappa-1} g_4\big(\mathscr{S}_h^{j-1}, \mathscr{V}_h^{j-1}, \mathscr{I}_h^{j-1}, \mathscr{R}_h^{j-1}, \mathscr{S}_v^{j-1}, \mathscr{I}_v^{j-1}, t_{j-1}\big),\\
T_j(\xi) &= \frac{\xi - t_{j-1}}{t_j - t_{j-1}} t_j^{\kappa-1} g_5\big(\mathscr{S}_h^j, \mathscr{V}_h^j, \mathscr{I}_h^j, \mathscr{R}_h^j, \mathscr{S}_v^j, \mathscr{I}_v^j, t_j\big)\\
&- \frac{\xi - t_j}{t_j - t_{j-1}} t_{j-1}^{\kappa-1} g_5\big(\mathscr{S}_h^{j-1}, \mathscr{V}_h^{j-1}, \mathscr{I}_h^{j-1}, \mathscr{R}_h^{j-1}, \mathscr{S}_v^{j-1}, \mathscr{I}_v^{j-1}, t_{j-1}\big),
\end{aligned}$$

$$\begin{aligned} U_j(\xi) &= \frac{\xi - t_{j-1}}{t_j - t_{j-1}} t_j^{\kappa-1} g_6\big(\mathscr{S}_h^j, \mathscr{V}_h^j, \mathscr{I}_h^j, \mathscr{R}_h^j, \mathscr{S}_v^j, \mathscr{I}_v^j, t_j\big) \\ &- \frac{\xi - t_j}{t_j - t_{j-1}} t_{j-1}^{\kappa-1} g_6\big(\mathscr{S}_h^{j-1}, \mathscr{V}_h^{j-1}, \mathscr{I}_h^{j-1}, \mathscr{R}_h^{j-1}, \mathscr{S}_v^{j-1}, \mathscr{I}_v^{j-1}, t_{j-1}\big). \end{aligned} \tag{16}$$

Thus, we have

$$\begin{aligned} \mathscr{S}_h^{m+1} &= \mathscr{S}_h^0 + \frac{\kappa}{\Gamma(\rho)} \sum_{j=0}^{m} \int_{t_j}^{t_{j+1}} \xi^{\kappa-1} (t_{m+1} - \xi)^{\rho-1} P_j(\xi) d\xi, \\ \mathscr{V}_h^{m+1} &= \mathscr{V}_h^0 + \frac{\kappa}{\Gamma(\rho)} \sum_{j=0}^{m} \int_{t_j}^{t_{j+1}} \xi^{\kappa-1} (t_{m+1} - \xi)^{\rho-1} Q_j(\xi) d\xi, \\ \mathscr{I}_h^{m+1} &= \mathscr{I}_h^0 + \frac{\kappa}{\Gamma(\rho)} \sum_{j=0}^{m} \int_{t_j}^{t_{j+1}} \xi^{\kappa-1} (t_{m+1} - \xi)^{\rho-1} R_j(\xi) d\xi, \\ \mathscr{R}_h^{m+1} &= \mathscr{R}_h^0 + \frac{\kappa}{\Gamma(\rho)} \sum_{j=0}^{m} \int_{t_j}^{t_{j+1}} \xi^{\kappa-1} (t_{m+1} - \xi)^{\rho-1} S_j(\xi) d\xi, \\ \mathscr{S}_v^{m+1} &= \mathscr{S}_v^0 + \frac{\kappa}{\Gamma(\rho)} \sum_{j=0}^{m} \int_{t_j}^{t_{j+1}} \xi^{\kappa-1} (t_{m+1} - \xi)^{\rho-1} T_j(\xi) d\xi, \\ \mathscr{I}_v^{m+1} &= \mathscr{I}_v^0 + \frac{\kappa}{\Gamma(\rho)} \sum_{j=0}^{m} \int_{t_j}^{t_{j+1}} \xi^{\kappa-1} (t_{m+1} - \xi)^{\rho-1} U_j(\xi) d\xi. \end{aligned} \tag{17}$$

Finally, the solution becomes as follows

$$\begin{aligned} \mathscr{S}_h^{m+1} &= \mathscr{S}_h^0 + \frac{\kappa h^\rho}{\Gamma(\rho+2)} \sum_{j=0}^{m} \Big[t_j^{\kappa-1} g_1\big(\mathscr{S}_h^j, \mathscr{V}_h^j, \mathscr{I}_h^j, \mathscr{R}_h^j, \mathscr{S}_v^j, \mathscr{I}_v^j, t_j\big) \times \\ &\Big[(m+1-j)^\rho (m-j+2+\rho) - (m-j)^\rho (m-j+2+2\rho) \Big] \\ &- t_{j-1}^{\kappa-1} g_1\big(\mathscr{S}_h^{j-1}, \mathscr{V}_h^{j-1}, \mathscr{I}_h^{j-1}, \mathscr{R}_h^{j-1}, \mathscr{S}_v^{j-1}, \mathscr{I}_v^{j-1}, t_{j-1}\big) \\ &\times \Big((m-j+1)^{\rho+1} - (m-j)^\rho (m-j+1+\rho) \Big) \Big], \\ \mathscr{V}_h^{m+1} &= \mathscr{V}_h^0 + \frac{\kappa h^\rho}{\Gamma(\rho+2)} \sum_{j=0}^{m} \Big[t_j^{\kappa-1} g_2\big(\mathscr{S}_h^j, \mathscr{V}_h^j, \mathscr{I}_h^j, \mathscr{R}_h^j, \mathscr{S}_v^j, \mathscr{I}_v^j, t_j\big) \times \\ &\Big[(m+1-j)^\rho (m-j+2+\rho) - (m-j)^\rho (m-j+2+2\rho) \Big] \\ &- t_{j-1}^{\kappa-1} g_2\big(\mathscr{S}_h^{j-1}, \mathscr{V}_h^{j-1}, \mathscr{I}_h^{j-1}, \mathscr{R}_h^{j-1}, \mathscr{S}_v^{j-1}, \mathscr{I}_v^{j-1}, t_{j-1}\big) \\ &\times \Big((m-j+1)^{\rho+1} - (m-j)^\rho (m-j+1+\rho) \Big) \Big], \\ \mathscr{I}_h^{m+1} &= \mathscr{I}_h^0 + \frac{\kappa h^\rho}{\Gamma(\rho+2)} \sum_{j=0}^{m} \Big[t_j^{\kappa-1} g_3\big(\mathscr{S}_h^j, \mathscr{V}_h^j, \mathscr{I}_h^j, \mathscr{R}_h^j, \mathscr{S}_v^j, \mathscr{I}_v^j, t_j\big) \times \end{aligned}$$

$$
\begin{aligned}
&\Big[(m+1-j)^{\rho}(m-j+2+\rho)-(m-j)^{\rho}(m-j+2+2\rho)\Big]\\
&-t_{j-1}^{\kappa-1}g_3\big(\mathscr{S}_h^{j-1},\mathscr{V}_h^{j-1},\mathscr{I}_h^{j-1},\mathscr{R}_h^{j-1},\mathscr{S}_v^{j-1},\mathscr{I}_v^{j-1},t_{j-1}\big)\\
&\times\Big((m-j+1)^{\rho+1}-(m-j)^{\rho}(m-j+1+\rho)\Big)\Big],\\
\mathscr{R}_h^{m+1} &= \mathscr{R}_h^{0}+\frac{\kappa h^{\rho}}{\Gamma(\rho+2)}\sum_{j=0}^{m}\Big[t_j^{\kappa-1}g_4\big(\mathscr{S}_h^{j},\mathscr{V}_h^{j},\mathscr{I}_h^{j},\mathscr{R}_h^{j},\mathscr{S}_v^{j},\mathscr{I}_v^{j},t_j\big)\times\\
&\Big[(m+1-j)^{\rho}(m-j+2+\rho)-(m-j)^{\rho}(m-j+2+2\rho)\Big]\\
&-t_{j-1}^{\kappa-1}g_4\big(\mathscr{S}_h^{j-1},\mathscr{V}_h^{j-1},\mathscr{I}_h^{j-1},\mathscr{R}_h^{j-1},\mathscr{S}_v^{j-1},\mathscr{I}_v^{j-1},t_{j-1}\big)\\
&\times\Big((m-j+1)^{\rho+1}-(m-j)^{\rho}(m-j+1+\rho)\Big)\Big],\\
\mathscr{S}_v^{m+1} &= \mathscr{S}_v^{0}+\frac{\kappa h^{\rho}}{\Gamma(\rho+2)}\sum_{j=0}^{m}\Big[t_j^{\kappa-1}g_5\big(\mathscr{S}_h^{j},\mathscr{V}_h^{j},\mathscr{I}_h^{j},\mathscr{R}_h^{j},\mathscr{S}_v^{j},\mathscr{I}_v^{j},t_j\big)\times\\
&\Big[(m+1-j)^{\rho}(m-j+2+\rho)-(m-j)^{\rho}(m-j+2+2\rho)\Big]\\
&-t_{j-1}^{\kappa-1}g_5\big(\mathscr{S}_h^{j-1},\mathscr{V}_h^{j-1},\mathscr{I}_h^{j-1},\mathscr{R}_h^{j-1},\mathscr{S}_v^{j-1},\mathscr{I}_v^{j-1},t_{j-1}\big)\\
&\times\Big((m-j+1)^{\rho+1}-(m-j)^{\rho}(m-j+1+\rho)\Big)\Big],\\
\mathscr{I}_v^{m+1} &= \mathscr{I}_v^{0}+\frac{\kappa h^{\rho}}{\Gamma(\rho+2)}\sum_{j=0}^{m}\Big[t_j^{\kappa-1}g_6\big(\mathscr{S}_h^{j},\mathscr{V}_h^{j},\mathscr{I}_h^{j},\mathscr{R}_h^{j},\mathscr{S}_v^{j},\mathscr{I}_v^{j},t_j\big)\times\\
&\Big[(m+1-j)^{\rho}(m-j+2+\rho)-(m-j)^{\rho}(m-j+2+2\rho)\Big]\\
&-t_{j-1}^{\kappa-1}g_6\big(\mathscr{S}_h^{j-1},\mathscr{V}_h^{j-1},\mathscr{I}_h^{j-1},\mathscr{R}_h^{j-1},\mathscr{S}_v^{j-1},\mathscr{I}_v^{j-1},t_{j-1}\big)\\
&\times\Big((m-j+1)^{\rho+1}-(m-j)^{\rho}(m-j+1+\rho)\Big)\Big]. \qquad (18)
\end{aligned}
$$

Theorem 2. *The fractal-fractional model* (2) *governing the dynamics of dengue infection has a unique solution.*

Proof. For the required proof, utilize the result of [35, 36], and take the Cauchy problem with power law as

$$\hbar(t)=\hbar(0)+\frac{\rho\kappa}{\Gamma(\rho)}\int_0^t \xi^{\kappa-1}g(\xi,\hbar(\xi))d\xi,$$

and introduce a map as follows

$$\Phi\theta(t)=\hbar(0)+\frac{\rho\kappa}{\Gamma(\rho)}\int_0^t \Phi^{\theta-1}g(\Phi,\psi(\xi))d\xi,$$

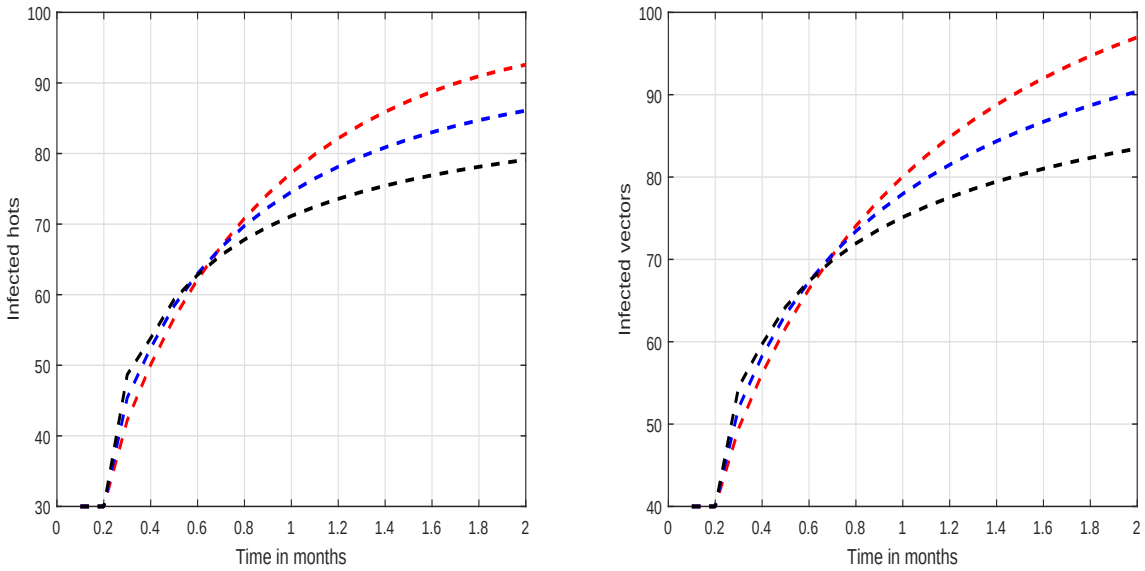

(a) (b)

Figure 1: The dynamics of infected individuals of system (2) of dengue fever with different fractional and fractal values while the values of other parameters are fixed.

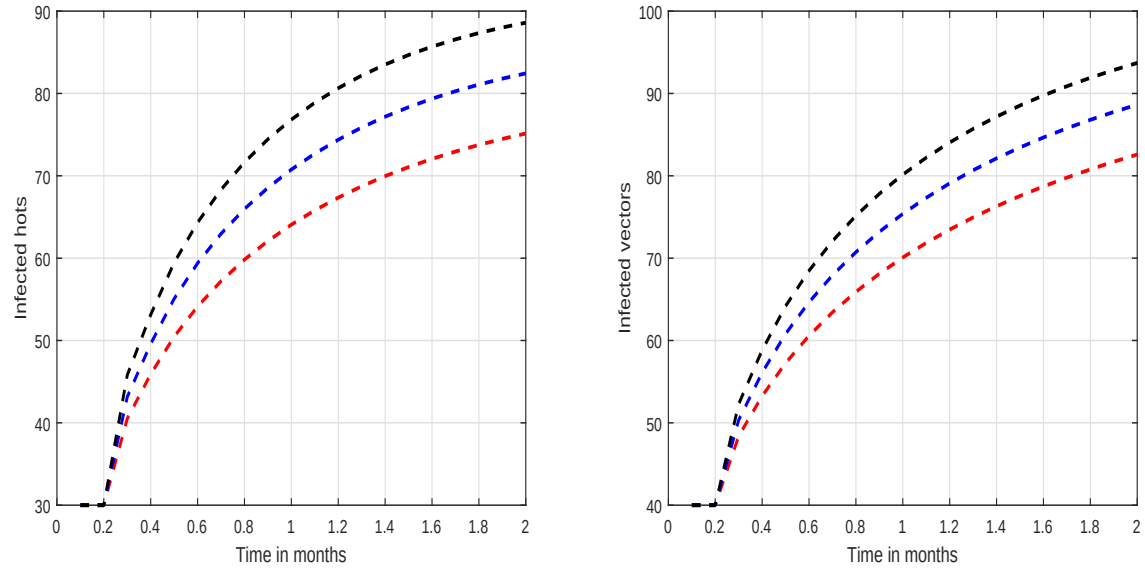

(a) (b)

Figure 2: The dynamics of infected individuals of system (2) of dengue fever with different values of b while the values of other parameters are fixed.

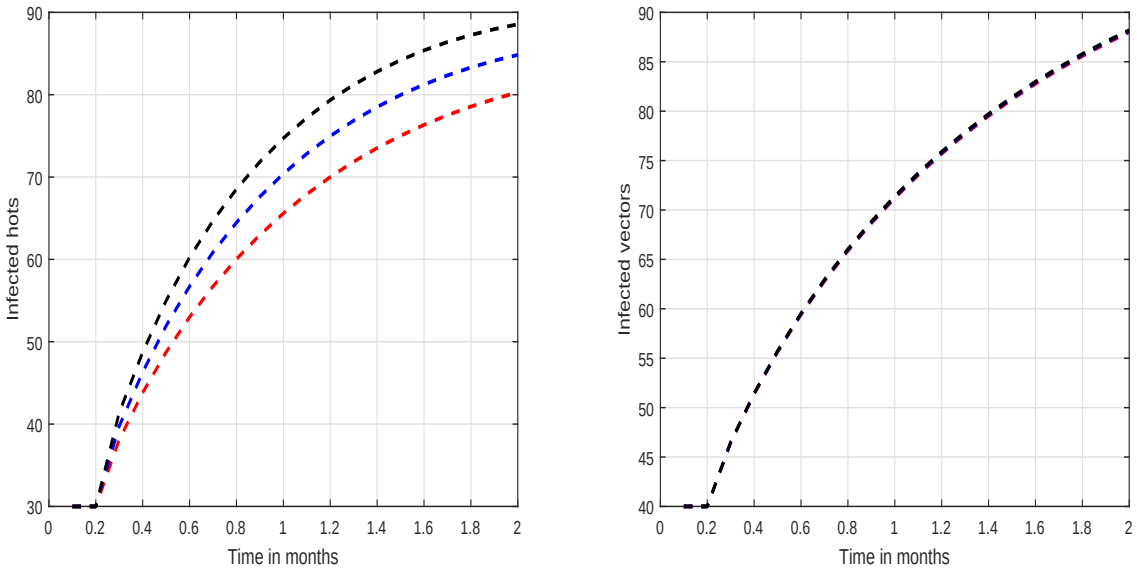

(a) (b)

Figure 3: The dynamics of infected individuals of system (2) of dengue fever with different values of β_1 while the values of other parameters are fixed.

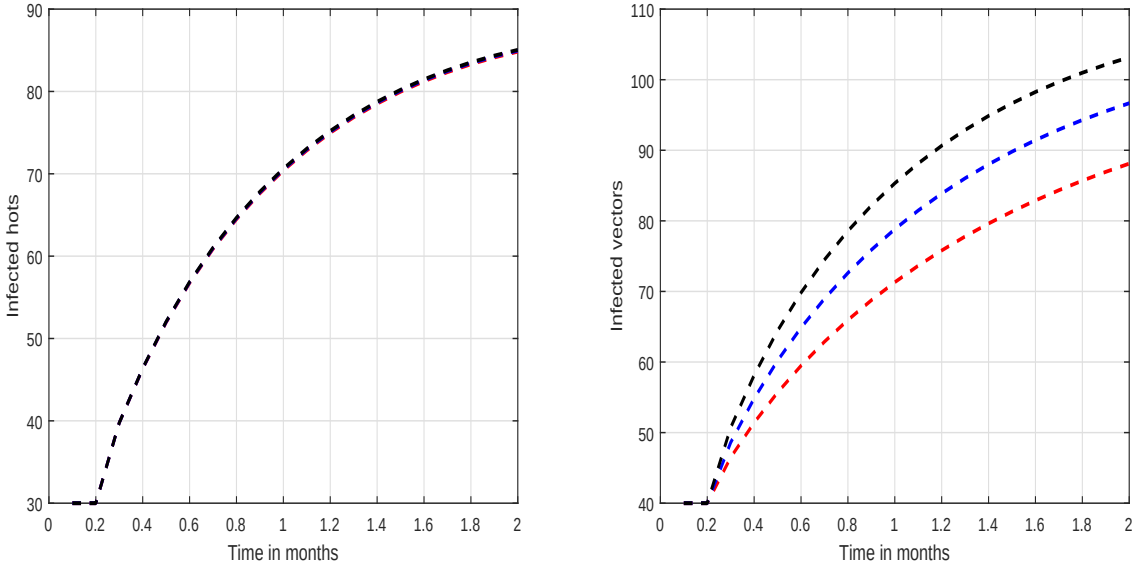

(a) (b)

Figure 4: The dynamics of infected individuals of system (2) of dengue fever with different values of β_3 while the values of other parameters are fixed.

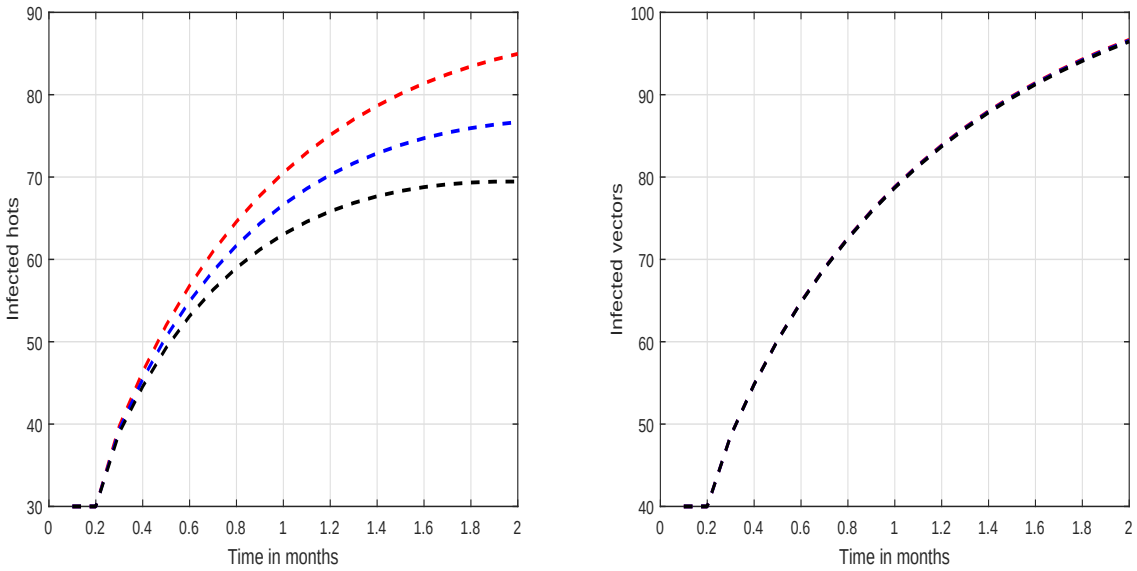

(a) (b)

Figure 5: The dynamics of infected individuals of system (2) of dengue fever with different rate of treatment while the values of other parameters are fixed.

which further gives

$$||\Phi\theta(t) - \hbar(0)|| < k \Longrightarrow V,$$

in which $V = \sup_{\Pi_e^c} |g|$ and $V < \frac{k\Gamma(\rho)}{\rho\kappa c^{\kappa+\rho-3}B(\kappa,\rho)}$.
Now, Take θ_1 and $\theta_2 \in C[I_n(t_n), A_e(t_n)]$, and determine the following

$$||\Phi\theta_1 - \Phi\theta_2|| < \frac{\rho\kappa L}{\Gamma(\rho)} c^{\kappa+\rho-3} B(\kappa,\rho).$$

As a result of this, one get the contractive property as

$$L < \frac{\Gamma(\rho)}{\rho\kappa c^{\kappa+\rho-3}B(\kappa,\rho)}.$$

In the case, if the above is obtained then we have

$$V < \frac{k\Gamma(\rho)}{\rho\kappa c^{\kappa+\rho-3}B(\kappa,\rho)},$$

thus, under power law the existence and uniqueness of the solution of the model has been proved and the proof is completed.

5. Results and discussions

Numerical simulations are essential for understanding the complex dynamics of epidemic models. These computational investigations enable the systematic exploration of disease transmission dynamics over time, offering insights into how infection trajectories evolve in response to varying initial states and parameter regimes. By employing numerical approaches, researchers can detect emergent phenomena including sustained oscillations, asymptotic stability, disease eradication, or endemic persistence. Such patterns are often governed by critical threshold parameters-most notably the basic reproduction number $\mathcal{R}_0$-that demarcate the boundary between epidemic outbreak and disease extinction. Moreover, numerical findings provide a unique window into the influence of biological memory, temporally varying control interventions, and intrinsic feedback mechanisms-features that are often analytically intractable within conventional modeling frameworks.

In essence, numerical experimentation complements and extends theoretical analysis, furnishing a robust platform for validating mathematical predictions, probing diverse epidemiological scenarios, and informing the design of effective disease mitigation strategies grounded in the model's long-term dynamical landscape. In this study, we performed a series of computational experiments to explore how variations in key biological and epidemiological parameters influence the spread of infection within a host-vector population. Initial conditions for the system's compartments-representing different population states-were carefully selected, and biologically plausible parameter values were used to simulate realistic transmission dynamics. This strategy enabled a thorough sensitivity analysis, shedding light on the roles of these parameters in shaping the temporal patterns of the epidemic.

In the first simulation, we investigated how modifications in the fractional and fractal derivative orders-which capture memory and heterogeneity effects in the system-affect the number of infected individuals over time, while maintaining all other parameters constant illustrated in Figure 1. The red curve represents the scenario where the fractional derivative order is 0.9 and the fractal order is 0.8; the blue curve corresponds to values of 0.8 and 0.7, respectively; and the black curve depicts the case with a fractional order of 0.7 and fractal order of 0.6. The results demonstrate that lower values of these orders are associated with a slower and more attenuated progression of the infection, suggesting that memory effects and spatial irregularities can significantly modulate the epidemic trajectory. Figure 2 illustrates the impact of the mosquito biting rate b on the infection dynamics, with all other parameters held fixed. The red, blue, and black curves correspond to biting rates of 0.45, 0.55, and 0.65, respectively. The simulation outcomes clearly indicate that an increase in the biting rate leads to a higher peak and faster rise in the number of infected individuals, underscoring the pivotal role of vector-host interactions in facilitating disease transmission. These findings highlight the biting rate as a key target for intervention strategies aimed at controlling vector-borne infections.

Figures 3 and 4 illustrate how variations in the transmission rates β_1 and β_3 influence the dynamics of the infected population. These findings highlight the critical role of transmission efficiency in shaping disease spread, where elevated values of β_1 and β_3

correspond to higher infection burdens within the host population. This suggests that increased contact or transmission potential significantly exacerbates the outbreak severity. Furthermore, Figure 5 explores the biological impact of the treatment rate τ on infection progression. The red, blue, and black trajectories represent treatment rates of 0.24, 0.34, and 0.44, respectively. As the treatment rate increases, a marked decline in the number of infected individuals is observed, indicating that enhanced treatment intervention can substantially suppress disease prevalence and support effective dengue control strategies within the community.

The proposed model and its associated simulations offer several significant advantages. Firstly, the incorporation of both fractional and fractal derivatives allows for the accurate characterization of memory and spatial heterogeneity effects, which are intrinsic to the dynamics of vector-borne diseases. This enhanced modeling framework captures long-range temporal dependence and spatial complexity more realistically than classical integer-order models. Secondly, the ability to vary key epidemiological parameters such as the biting rate, transmission coefficients, and treatment efficacy facilitates a comprehensive sensitivity analysis and helps identify the critical factors that drive disease transmission. Thirdly, the simulations provide valuable insights into the nonlinear behavior of the system under different parameter regimes, facilitating the assessment of intervention strategies such as increased treatment rates or vector control measures. Lastly, the model's general structure allows it to be extended or adapted to other infectious diseases with comparable transmission patterns, making it a valuable and versatile tool for informing public health policies and control strategies.

6. Conclusions

In this study, we developed a novel fractal-fractional mathematical framework based on the Caputo operator to describe the intricate biological processes underlying dengue fever transmission. The model integrates key biological features such as vaccination, treatment and saturation effects in infection rates, reflecting the limited capacity of vectors to transmit the virus under high infectious pressure. The biological soundness of the model was ensured by demonstrating that population compartments remain positive and bounded over time, preserving epidemiological realism. The calculation of the basic reproduction number $\mathcal{R}_0$ provided a biologically meaningful threshold indicator, distinguishing between disease extinction and persistence. Through biologically informed numerical simulations, we explored how variations in vaccination, transmission intensity, treatment rate and vector infectivity influence the spread of dengue. The simulations highlighted the importance of timely immunization and targeted vector control in curbing infection prevalence. Our results underscore the potential of fractional-order models to capture memory effects and biological heterogeneity in disease dynamics, offering valuable guidance for designing effective public health interventions to control dengue outbreaks in endemic and high-risk regions. These findings not only enhanced theoretical understanding but also offered practical implications by identifying influential control variables. In our future work, we aim to investigate the impact of time delays on the dynamics of dengue infection, thereby

capturing the influence of latency periods more effectively.

References

[1] R. Dehghani and H. Kassiri. A review on epidemiology of dengue viral infection as an emerging disease. *Research Journal of Pharmacy and Technology*, 14(4):2296–2301, 2021.

[2] M. S. Abdullah, M. J. Islam, M. M. Hasan, D. Sarkar, M. S. Rana, S. S. Das, and M. Hossian. Impact of waste management on infectious disease control: Evaluating strategies to mitigate dengue transmission and mosquito breeding sites–a systematic review. *Journal of Angiotherapy*, 8(8):1–12, 2024.

[3] E. Y. Y. Chan, T. S. T. Sham, T. S. Shahzada, C. Dubois, Z. Huang, S. Liu, K. K. Hung, S. L. Tse, K. O. Kwok, P. H. Chung, and R. Kayano. Narrative review on health-edrm primary prevention measures for vector-borne diseases. *International Journal of Environmental Research and Public Health*, 17(16):5981, 2020.

[4] Susie East. World's first dengue fever vaccine launched in the philippines, 2016. CNN, 6 April 2016. Archived from the original on 18 October 2016. Retrieved 17 October 2016.

[5] Epidemiology. www.cdc.gov/dengue/epidemiology/index.html. Retrieved 7 March 2018.

[6] M. A. Johansson, J. Hombach, P. Sinha, and D. A. Cummings. Models of the impact of dengue vaccines: A review of current research and potential approaches. *Vaccine*, 29(35):5860–5868, 2011.

[7] J. G. Julander, S. T. Perry, and S. Shresta. Important advances in the field of anti-dengue virus research. *Antiviral Chemistry & Chemotherapy*, 21(3):105–116, 2011.

[8] H. Medekhel, R. Jan, S. Boulaaras, R. Guefaifia, and A. Himadan. Existence and uniqueness of solutions to a weighted laplace equation with spectral perturbation near a plane sector vertex. *Fractals*, page 2540178, 2025.

[9] M. Ramzan, A. Shafique, S. Abbas, R. Ali, T. Lamoudan, R. Jan, M. Norberdiyeva, B. Turabova, and H. A. S. Garalleh. Mathematical analysis of prandtl number with artificial neural network and fractional operator for nanofluid flow. *Case Studies in Thermal Engineering*, page 106164, 2025.

[10] Z. Khan, M. Jawad, E. Bonyah, N. Khan, and R. Jan. Magnetohydrodynamic thin film flow through a porous stretching sheet with the impact of thermal radiation and viscous dissipation. *Mathematical Problems in Engineering*, 2022(1):1086847, 2022.

[11] M. C. Bahi, S. Bahramand, R. Jan, S. Boulaaras, H. Ahmad, and R. Guefaifia. Fractional view analysis of sexual transmitted human papilloma virus infection for public health. *Scientific Reports*, 14(1):3048, 2024.

[12] R. Jan and Y. Xiao. Effect of pulse vaccination on dynamics of dengue with periodic transmission functions. *Advances in Difference Equations*, 2019(1):1–17, 2019.

[13] R. Jan, Z. Shah, W. Deebani, and E. Alzahrani. Analysis and dynamical behavior of a novel dengue model via fractional calculus. *International Journal of Biomathematics*, 15(06):2250036, 2022.

[14] L. Esteva and C. Vargas. Analysis of a dengue disease transmission model. *Mathematical Biosciences*, 150(2):131–151, 1998.

[15] L. Esteva and C. Vargas. A model for dengue disease with variable human population. *Journal of Mathematical Biology*, 38(3):220–240, 1999.

[16] M. Derouich, A. Boutayeb, and E. H. Twizell. A model of dengue fever. *Biomedical Engineering Online*, 2:1–10, 2003.

[17] R. Jan and Y. Xiao. Effect of partial immunity on transmission dynamics of dengue disease with optimal control. *Mathematical Methods in the Applied Sciences*, 42(6):1967–1983, 2019.

[18] Z. Feng and J. X. Velasco-Hernández. Competitive exclusion in a vector-host model for the dengue fever. *Journal of Mathematical Biology*, 35:523–544, 1997.

[19] N. Nuraini, E. Soewono, and K. A. Sidarto. Mathematical model of dengue disease transmission with severe dhf compartment. *Bulletin of the Malaysian Mathematical Sciences Society*, 30(2), 2007.

[20] J. J. Tewa, J. L. Dimi, and S. Bowong. Lyapunov functions for a dengue disease transmission model. *Chaos, Solitons & Fractals*, 39(2):936–941, 2009.

[21] R. Jan, S. Boulaaras, S. Alyobi, K. Rajagopal, and M. Jawad. Fractional dynamics of the transmission phenomena of dengue infection with vaccination. *Discrete and Continuous Dynamical Systems - Series S*, 2022.

[22] S. M. C. Tirado and K. J. Yoon. Antibody-dependent enhancement of virus infection and disease. *Viral Immunology*, 16(1):69–86, 2003.

[23] L. Billings, A. Fiorillo, and I. B. Schwartz. Vaccinations in disease models with antibody-dependent enhancement. *Mathematical Biosciences*, 211(2):265–281, 2008.

[24] K. W. Blayneh, A. B. Gumel, S. Lenhart, and T. Clayton. Backward bifurcation and optimal control in transmission dynamics of west nile virus. *Bulletin of Mathematical Biology*, 72(4):1006–1028, 2010.

[25] D. Moulay, M. A. Aziz-Alaoui, and M. Cadivel. The chikungunya disease: Modeling, vector and transmission global dynamics. *Mathematical Biosciences*, 229(1):50–63, 2011.

[26] D. Aldila, T. Götz, and E. Soewono. An optimal control problem arising from a dengue disease transmission model. *Mathematical Biosciences*, 242(1):9–16, 2013.

[27] H. S. Rodrigues, M. T. Monteiro, and D. F. Torres. Vaccination models and optimal control strategies to dengue. *Mathematical Biosciences*, 247:1–12, 2014.

[28] W. O. Dias, E. F. Wanner, and R. Cardoso. A multi objective optimization approach for combating aedes aegypti using chemical and biological alternated step-size control. *Mathematical Biosciences*, 269:37–47, 2015.

[29] R. Jan, Z. Shah, N. Vrinceanu, M. H. Alshehri, N. N. A. Razak, and M. Racheriu. Fractional view analysis of the dynamics of a plant disease through caputo–fabrizio derivative. *Fractals*, page 2540079, 2025.

[30] R. Jan, N. N. A. Razak, M. Alrawashdeh, A. Alharbi, V. T. Pham, and M. Mousa. Analysis of the dynamics of hiv and the immune system under the effect of drugs through a fractional framework. *Fractals*, page 2540148, 2025.

[31] Z. Shah, N. Ullah, R. Jan, M. H. Alshehri, N. Vrinceanu, E. Antonescu, and

M. Farhan. Existence and sensitivity analysis of a caputo-fabrizio fractional order vector-borne disease model. *European Journal of Pure and Applied Mathematics*, 18(2):5687–5687, 2025.

[32] S. Abbas, S. Saleem, M. Fatima, I. L. Popa, M. Nazar, G. R. Elnaggar, and R. Jan. Slip and thermal effects on mhd fractional jeffrey nanofluid flow. *Journal of Radiation Research and Applied Sciences*, 18(3):101688, 2025.

[33] I. Ahmad, R. Jan, N. N. A. Razak, A. Khan, and T. Abdeljawad. Numerical investigation of the dynamical behavior of hepatitis b virus via caputo-fabrizio fractional derivative. *European Journal of Pure and Applied Mathematics*, 18(1):5509–5509, 2025.

[34] Z. U. Rehman, S. Boulaaras, R. Jan, I. Ahmad, and S. Bahramand. Computational analysis of financial system through non-integer derivative. *Journal of Computational Science*, 75:102204, 2024.

[35] A. Atangana. Fractal-fractional differentiation and integration: Connecting fractal calculus and fractional calculus to predict complex system. *Chaos, Solitons & Fractals*, 102:396–406, 2017.

[36] A. Atangana and S. Qureshi. Modeling attractors of chaotic dynamical systems with fractal-fractional operators. *Chaos, Solitons & Fractals*, 123:320–337, 2019.

[37] R. Jan, M. A. Khan, and J. F. Gómez-Aguilar. Asymptomatic carriers in transmission dynamics of dengue with control interventions. *Optimal Control Applications and Methods*, 41(2):430–447, 2020.

[38] S. Boulaaras, M. Yavuz, Y. Alrashedi, S. Bahramand, and R. Jan. Modeling the co-dynamics of vector-borne infections with the application of optimal control theory. *Discrete and Continuous Dynamical Systems - Series S*, 18(5):1331–1352, 2025.